

First-principles study of nonclassical effects in silicon-based nanocapacitors

Hiroyuki Kageshima* and Akira Fujiwara

NTT Basic Research Laboratories, NTT Corporation, 3-1 Morinosato-Wakamiya, Atsugi, Kanagawa 243-0198, Japan

(Received 2 January 2012; revised manuscript received 3 April 2012; published 4 May 2012)

Properties of silicon-based nanocapacitor are studied from first principles. The nanocapacitor consists of electrodes of the silicon-based material planar polysilane. Nonclassical effects are analyzed by changing both the electrode spacing and the applied bias simultaneously. Even when the electrode spacing is fixed, the effective electrode spacing decreases with applied bias because of the quantum capacitance effect. In addition, when the electrostatic capacitance is analyzed in detail, it is also found that the effective electrode surface changes complicatedly with electrode spacing and applied bias because of the dielectric polarization effect of the electrode material. The dielectric polarization effect is one order of the magnitude smaller than the quantum capacitance effect, which is due to the nature of the electrode material, planar polysilane. It is clarified that a nanocapacitor is governed by the detailed properties of the electronic states of the electrode materials as well as the geometry.

DOI: 10.1103/PhysRevB.85.205304

PACS number(s): 68.60.-p, 85.35.-p

I. INTRODUCTION

The physical properties of nanoscale structures are attracting great interest, and various new phenomena have been discovered. Since any field effect transistor with nanostructures acts as a nanocapacitor, an understanding of the physical properties of a nanocapacitor is important. In classical electrostatics, the capacitance is geometrically determined by the electrode spacing and the dielectric constant between the electrodes. However, the capacitance of nanocapacitors is not so simple. It is known that quantum capacitance plays an important role in nanocapacitors.¹⁻¹⁰ The capacitance C of a nanocapacitor is written as

$$C = \frac{1}{1/C_{es} + 1/C^+ + 1/C^-}, \quad (1)$$

where C_{es} is the geometric capacitance, and C^+ and C^- are the quantum capacitances of the positive electrode and of the negative electrode, respectively.^{1,7} Since the quantum capacitance originates from the density of states of the electrodes, the electronic structure of the electrodes is reflected in the capacitance. Recent progress in nanofabrication techniques have made experimental observations of such quantum capacitance possible. Van Hove singularity of the density of states has been clearly observed for a carbon nanotube nanocapacitor.¹¹ It has also been revealed that the device properties of a graphene field effect transistor are governed by the quantum capacitance.^{12,13}

The physical properties of nanocapacitors have also been studied theoretically.¹⁴⁻²³ Equation (1) is extended for the case of the single channel contact with leakage current as

$$C = \frac{R}{1/C_{es} + 1/C^+ + 1/C^-}, \quad (2)$$

where R is the reflecting probability of the contact.¹⁴ A clear quantum capacitance has been reported for nanocapacitors based on electrodes made of materials like SrTiO₃ and carbon nanotube. In addition, the theories also show another nonclassical behavior of nanocapacitors: The effective electrode distance is shorter than the real geometrical distance for the ideal jellium nanocapacitor while the quantum capacitance effect cannot appear.¹⁷ This is attributed to the electron spill out from the electrodes by the dielectric polarization effect.

Generally speaking, when a bias is applied, charging on the electrodes and electric field between the electrodes induce dielectric polarization in the electrode materials. Because of this polarization, C_{es} , C^+ , and C^- must be disturbed by the applied bias, and nonclassical phenomena such as electron spillout occur.

This suggests that the physical property of nanocapacitors is also affected by the dielectric polarization, while the detail has not been sufficiently clarified yet. In this study, we therefore investigate the relation of the dielectric polarization effect with the quantum capacitance effect in nanocapacitors with realistic electrodes consisting of atoms based on the first-principles approach. We focus on the electronic polarization effect among the dielectric polarization effect, and neglect the lattice polarization effect.

Here, we study a nanocapacitor with planar polysilane electrodes. Planar polysilane is a silicon (Si) atomic sheet with surface hydrogen (H) termination²⁴⁻²⁶ [Fig. 1(a)]. It is two-dimensional and semiconducting with the band gap of 2.21 eV. It is the ultimate structure of silicon (111) thin film and a prototype of silicon nanodevices, which have been discussed as a light-emitting silicon.^{27,28} Because of surface H termination and strong quantum confinement normal to the plane, it is difficult to be polarized dielectrically as shown in its normal dielectric constant about 6.5 lower than that of bulk Si (about 14) or of ideal metal (∞).²⁹ In addition, since the two-dimensional semiconductor feature results in a step-function-like square density of states, large and clear quantum capacitance is expected. We study both the electrode-spacing dependence and applied-bias dependence simultaneously to clarify the physical properties of the nanocapacitor and confirm nonclassical features for the nanocapacitance coming from the dielectric polarization of the electrode materials as well as from the quantum capacitance.

II. METHOD

As the electrodes of the capacitor, we employ planar polysilane. The area of the lateral unit cell is 12.76 Å². The atomic layer spacings of Si-H and Si-Si in the electrode are 1.50 and 0.74 Å. The thickness of the electrode is then 3.74 Å if the surfaces are determined by the position of the H atoms. Therefore, the distances from the center of the electrode to

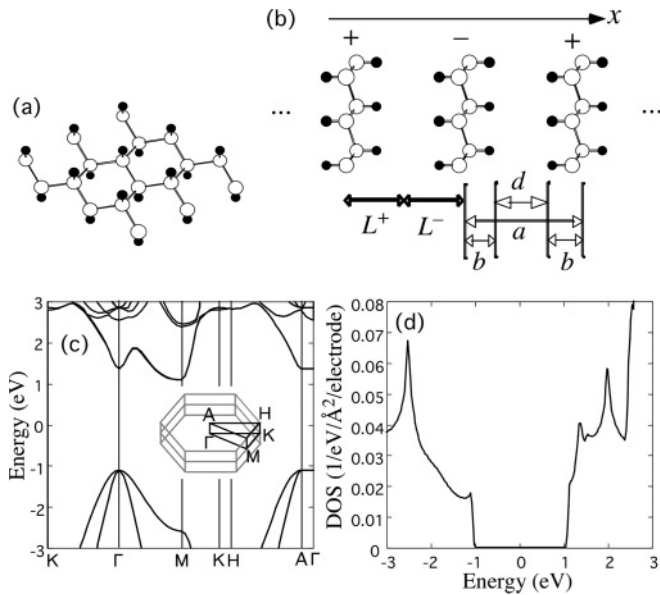


FIG. 1. Atomic structures and fundamental properties of the calculated nanocapacitor. (a) Close-up view of the atomic structure of the electrode, planar polysilane. (b) Side view of the nanocapacitor. Solid and empty circles indicate H and Si atoms, respectively. (c) Band dispersion relation of the noncharged electrode. (d) Density of states of the noncharged electrode.

the H atom for both the positive and negative electrodes [b in Fig. 1(b)] are 1.87 Å. Our model capacitor is made of an infinite superlattice alternation of such polysilanes with fixed spacing. Alternative bias application makes the electrodes positively and negatively charged one by one [Fig. 1(b)].

We apply bias on the electrodes of the capacitors and calculate the electronic states and the accumulated charge from first principles using the enforced Fermi energy difference (EFED) method we have developed.^{19,29,30} This EFED method enables us to apply a relatively high bias between the electrodes, because the method prohibits the flow of the leakage current between the electrodes. This means that R in Eq. (2) is kept as 1 even under application of a high bias. We used norm-conserving pseudopotentials, the plane-wave basis set to the cutoff of 25 Ry, the generalized gradient approximation (GGA) with the exchange-correlation functional,³¹ and 72 sample k points in the first Brillouin zone. For simplicity of the discussion and the analysis, the atomic positions are fixed even when bias is applied. We also just consider the zero electronic temperature case. To make the analysis of quantum capacitance easier, we use relatively short 4.76, 5.46, 6.58, or 7.94 Å as the electrode spacing, d , the distance between the surface H layers of the positive and the negative electrode. Since we apply the bias μ from zero to 8.2 eV, the electric field between the electrodes achieves the order of 1×10^{10} V/m in the maximum.

As shown in the band dispersion relation for the nonbiased case [Fig. 1(c)], the electrodes are semiconducting with the indirect band gap E_g of 2.21 eV. Since the confinement is along the [111] direction, all electron pockets in the conduction band bottom are projected on the points between Γ and M . Since we do not consider the spin-orbit interaction, the valence band top at the Γ point is doubly degenerated. At the Γ point of

the conduction band bottom, a pocket also appears due to the antibonding of the surface-terminated Si-H bonds. The direct band gap at the Γ point is, then, 2.48 eV. The flat dispersion in the direction perpendicular to the Si plane indicates that the electronic states of the electrodes are well-separated by the vacuum between them. The density of states for the nonbiased case shows a step-function-like square feature at both the conduction and the valence band edges, as expected from the two-dimensional atomic structure. It also shows a larger value at the conduction band edge than at the valence band edge [Fig. 1(d)]. This is because the bottom of the conduction band is six-times degenerated, while the top of the valence band is doubly degenerated. The band structure indicates that electrons accumulate in the conduction band bottom at the M point in the negative electrode, while holes accumulate in the valence band top at the Γ point in the positive electrode.

III. CHARGE ACCUMULATION

When a bias μ is applied, positive and negative charges accumulate on the positive electrode and the negative electrode, respectively. The absolute value of the accumulated areal charge on the electrode Q can be evaluated as follows:

$$Q = \left| \int_{L_+} \Delta\rho(x) dx \right|. \quad (3)$$

Here $\Delta\rho(x)$ represents the laterally averaged distribution at x of the increase in the electron density from the $\mu = 0$ case. The integral section, L_+ , starts from the center of the positive electrode and ends at the middle of the two electrodes [Fig. 1(b)].

$\Delta\rho(x)$ on the positive electrode and on the negative electrode are shown as the function of x position for various μ for $d = 7.94$ Å in Figs. 2(a) and 2(b). Since holes and electrons

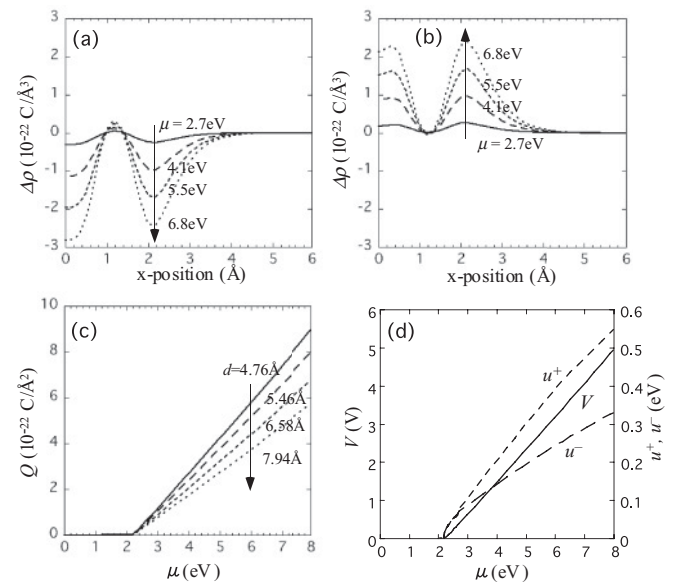


FIG. 2. Changes in the electron density $\Delta\rho(x)$ at $d = 7.94$ Å on (a) the positive electrode and (b) the negative electrode as a function of x position for various applied biases μ . (c) Accumulated charge Q as a function of applied bias μ . (d) Extracted V , u^- , and u^+ as a function of μ .

are accumulated in the valence band of the positive electrode and the conduction band of the negative electrode, respectively, $\Delta\rho(x)$ of the negative electrode shows a different shape from that of the positive electrode. Such a difference causes a nonclassical effect on the nanocapacitance, as discussed below.

The calculated Q is shown in Fig. 2(c) as a function of μ and d . The charge accumulation occurs when $\mu > E_g$. This is because electrons at the top of the valence band of the positive electrode cannot move into the conduction band bottom on the negative electrode due to the band gap of the semiconducting electrodes if μ is smaller than the band gap E_g . Figure 2(c) also shows that Q decreases as d increases. This can be explained by the weakening of the electric field due to the increase of d as in the classical theory.

The applied bias μ should not be confused with the electrostatic potential difference V (see Fig. 4 in Ref. 19). When a bias is applied, electrons accumulate in the conduction band bottom and holes accumulate in the valence band top. A part of the bias is used as the increase of the Fermi energies in the electrode, u^+ and u^- . μ is therefore the sum of the band gap E_g and the electrostatic potential V in addition to u^+ and u^- :

$$\mu = E_g + eV + u^+ + u^-. \quad (4)$$

Here e is the elementary charge. Thus, we decompose μ into each contribution of u^+ , u^- , and V from the change of the eigenenergies of the calculated electronic states as μ changes [Fig. 2(d)]. The results indicate that the contributions of u^+ and u^- are smaller by one order of magnitude than that of V and too large to be neglected.

IV. CAPACITANCE AND QUANTUM CAPACITANCE

The areal capacitance C can be calculated as $C = edQ/d\mu$. The calculated capacitances look like a step function, while they slowly increase for $\mu > E_g$ [Fig. 3(a)]. The increase

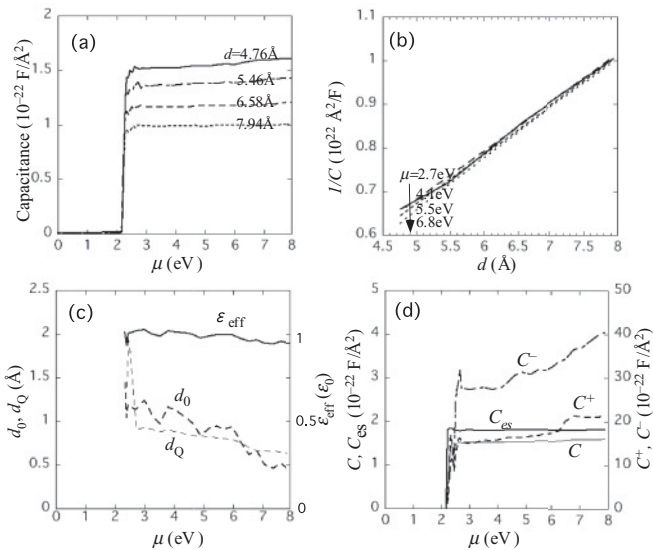


FIG. 3. (a) Capacitance C as the function of applied bias μ . (b) Capacitance C at fixed μ as a function of d . (c) Effective permittivity ϵ_{eff} and effective residual electrode spacing d_0 as a function of μ . (d) Comparison of C with its components C_{es} , C^+ , and C^- as a function of μ .

is more rapid for smaller d . They also simply decrease as d increases, which is consistent with the classical theory.

If we plot $1/C$ as a function of d , the relationship appears to be linear, as shown in Fig. 3(b), while it has weak dependence on μ . We then fit the d dependence of C for each μ by $C = \epsilon_{\text{eff}}/(d + d_0)$ with fitting parameters ϵ_{eff} and d_0 when $\mu > E_g$. The result is shown in Fig. 3(c). It is clear that the capacitance C shows nonclassical features. The effective residual electrode spacing d_0 drastically decreases with increasing μ , while the positive values of d_0 indicate that the effective electrode surfaces are located between H and Si layers. On the other hand, the effective permittivity ϵ_{eff} stays around its ideal value of ϵ_0 , while it slightly decreases when μ increases. This means that Eq. (2) with $R = 1$ is surely satisfied in our results as we expected.

To clarify the reason of such nonclassical features, we decompose C into electrostatic and quantum capacitances. If we recall Eq. (4), $C = edQ/d\mu$ is written as

$$\frac{1}{C} = \frac{1}{C_{\text{es}}} + \frac{1}{C^+} + \frac{1}{C^-}. \quad (5)$$

This is the same form as Eq. (1). Here, $C_{\text{es}} = dQ/dV$ is the geometric capacitance, or the electrostatic capacitance. $C^+ = edQ/du^+$ and $C^- = edQ/du^-$ are the quantum capacitances of the positive electrode and the negative electrode, respectively. The three components for $d = 4.76 \text{ \AA}$ are evaluated from the results shown in Fig. 2(c) as a function of μ [Fig. 3(d)]. The absolute values of quantum capacitances C^+ and C^- are larger by one order of magnitude than those of capacitance C and electrostatic capacitance C_{es} . This is because the contributions of u^+ and u^- are smaller by one order of magnitude than that of eV .

Since u^+ and u^- are the Fermi energy positions in the electrodes, the quantum capacitances can be written as $C^+ = eD^+/2$ and $C^- = eD^-/2$ by using the electrode density of states D^+ and D^- . The factors 1/2 on the right-hand side come from the periodic geometry of our system. We can evaluate $D^+ = 0.019 \text{ eV}^{-1} \text{ \AA}^{-2}$ and $D^- = 0.035 \text{ eV}^{-1} \text{ \AA}^{-2}$ at $\mu = 3.0 \text{ eV}$. These values show good consistency with the electrode density of states for $\mu = 0$ shown in Fig. 1(d). D^+ and D^- correspond to the density of states at the valence band top and conduction band bottom, respectively. In addition, the μ dependence of C^+ and C^- is also consistent with the density of states shown in Fig. 1(d).

On the other hand, C_{es} stays almost constant but slightly increases when $\mu > E_g$ [Fig. 3(d)]. This indicates that the increase in C with increasing μ mainly comes from the increase in C^+ and C^- . This means that the μ dependence of d_0 mainly comes from that of quantum capacitances C^+ and C^- , if we recall $C = \epsilon_{\text{eff}}/(d + d_0)$. The contribution from C^+ and C^- to d_0 can be evaluated by $d_0 = \epsilon_0(1/C^+ + 1/C^-)$. The obtained d_0 for $d = 4.76 \text{ \AA}$ is consistent with d_0 [Fig. 3(c)]. This suggests that d_0 can be mostly explained by the effect of the quantum capacitance even for a relatively high bias.

It should be noted here that D^+ and D^- shown in Fig. 3(d) are, rigorously speaking, different from the density of states shown in Fig. 1(d). Since bias is applied for D^+ and D^- , they are affected by the dielectric polarization of the electrode

materials. It seems that the slight decrease in ϵ_{eff} with the increase in μ is also the result of the dielectric polarization.

V. ELECTROSTATIC CAPACITANCE

Next, we analyze the electrostatic capacitance C_{es} in detail and discuss the dielectric polarization effect on C_{es} . In the classical picture, this part is thought to be determined solely by the geometry of the electrodes. From the geometrical point of view, the electrostatic potential V can be described as

$$V = \frac{Q}{\epsilon_0}(a - d_{\text{es}}^+ - d_{\text{es}}^-). \quad (6)$$

Here $a = d + 2b$, as shown in Fig. 1(b). Effective electrode surface distances d_{es}^{\pm} are defined by

$$d_{\text{es}}^{\pm} = \frac{1}{Q} \left| \int_{L_{\pm}} \Delta\rho(x)(x - x_0^{\pm})dx \right|, \quad (7)$$

where x_0^{\pm} is the x position of the center of the positive electrode (+) or the negative electrode (-). $\Delta\rho(x)$ is the laterally averaged distribution at x of the increase in the electron density from the $\mu = 0$ case [Figs. 2(a) and 2(b)]. The integral section, L_{\pm} , starts from the center of the electrode, positive electrode (+) or negative electrode (-), and ends at the middle of the two electrodes [Fig. 1(b)]. Using this d_{es}^{\pm} , $C_{\text{es}} = dQ/dV$ can be written as

$$C_{\text{es}} = \frac{\epsilon_0}{a - d_{\text{es}}^+ - d_{\text{es}}^-} \quad (8)$$

if we assume that d_{es}^{\pm} does not depend on Q or μ as in the classical picture. Alternatively, using $d_{\text{es}} = 2b - d_{\text{es}}^+ - d_{\text{es}}^-$, C_{es} can be written as

$$C_{\text{es}} = \frac{\epsilon_0}{d + d_{\text{es}}}. \quad (9)$$

Therefore, analyzing d_{es}^{\pm} or d_{es} leads us to a detailed discussion of the physical properties of C_{es} .

The calculated d_{es}^{\pm} for our nanocapacitor are shown in Fig. 4(a) as a function of μ . The results indicate that electrode surface differs between the positive electrode and the negative electrode and moves with μ and d on the order of 0.1 Å. This means that, strictly speaking, the classical understanding of the electrostatic capacitance is not appropriate for our nanocapacitor. The μ dependence of d_{es}^+ and d_{es}^- for $d = 4.76$ Å has already been discussed in our previous work,^{29,30} where we compared the changes of d_{es}^+ and d_{es}^- with those calculated from the wave functions around the Fermi energy. We discussed that the relatively high changes of d_{es}^+ and d_{es}^- come from the μ -dependence nature of the dielectric response of the electrode materials. In this study, however, we discuss d_{es}^+ and d_{es}^- more deeply in terms of physics to clarify the effect of the dielectric polarization on the electrode materials.

The figure indicates that d_{es}^+ decreases for $\mu > 3$ eV as μ increases, while it first increases. On the other hand, d_{es}^- increases for $\mu > 3$ eV as μ increases, while it first decreases. The μ dependence for the positive electrode is thus opposite to that for the negative electrode. This relation holds for any d . We hereafter focus on the range of $\mu > 3$ eV, because the error in the calculation is considered to be large for $\mu < 3$ eV since

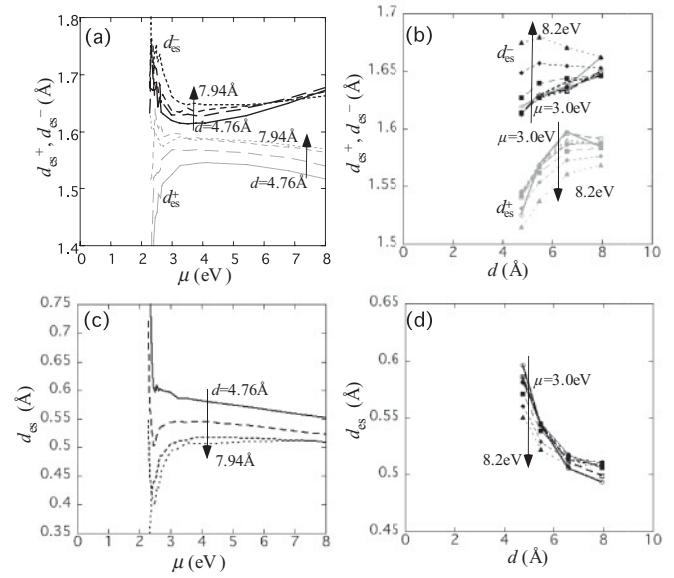


FIG. 4. Effective electrode surface distances d_{es}^{\pm} as a function of (a) applied bias μ and (b) electrode spacing d . d_{es} as a function of (c) applied bias μ and (d) electrode spacing d .

only little charge Q accumulates on the electrodes. It is thought that the change of μ affects both the charge Q accumulated on the electrodes and the electric field E induced between them. This leads us to discuss the μ -dependent results in terms of the effects of Q and E .

First, we consider the dielectric polarization effect coming from Q . On the nanoscale, the electrode consists of atomic nuclei and electrons, and the change of Q comes from the change of the total number of electrons on the electrode. The total number of electrons increases on the negative electrode, while it decreases on the positive electrode. Since the amount of positive background of the nuclei does not change, the Coulomb force more attracts the electrons for the positive electrode and repulses them for the negative electrode. Therefore, the increase of Q is considered to result in the decrease of d_{es}^+ and the increase of d_{es}^- .

Next, we consider the dielectric polarization effect coming from E . Since the opposite charge is located on the opposite electrode, E has an effect of separating the positive charge from the positive electrode and the negative charge from the negative electrode. On the nanoscale, E attracts the electrons for the positive electrode and repulses the electrons from the electrode for the negative electrode. Therefore, the increase of E is considered to result in the decrease of d_{es}^+ and the increase of d_{es}^- . The increase of E thus has the same effect as the increase of Q . In classical electrostatics, Q is proportional to E . This is consistent with the discussions here. Since the increase of μ results in the increase of both Q and E , these discussions indicate that d_{es}^+ decreases and d_{es}^- increases when μ increases. This is surely consistent with the calculated behaviors of d_{es}^+ and d_{es}^- for $\mu > 3$ eV shown in Fig. 4(a).

In this study, we also successfully calculated the d dependence of d_{es}^{\pm} , as shown in Fig. 4(b). The d_{es}^{\pm} are also shown in Fig. 4(b) as a function of d for each of fixed μ . These figures show that both d_{es}^{\pm} are monotonically increasing functions of d except for d_{es}^- with $\mu > 7$ eV. The d dependence can also be

discussed in terms of the dielectric polarization effect by the changes of Q and E . According to classical electrostatics, both Q and E increase in proportional to $1/d$ as d increases with fixing μ . This means that the decrease of d plays the same role as the increase of μ . This explains almost all calculated results on the d dependence shown in Figs. 4(a) and 4(b), while it fails to explain the d dependence of d_{es}^- for $\mu < 7$ eV.

The reason for the unexpected behavior of d_{es}^- for $\mu < 7$ eV is thought to be an artifact of our EFED method. In the EFED method, electrons in the negative electrode are artificially trapped in an additional well with μ -dependent depth. The width of the well also changes with d . When d is smaller, electrons in the negative electrode are trapped more tightly around the center of the electrode. Here, we should note that d_{es}^+ is not affected by this artifact. If the EFED artifact had the effect, the electrons in the positive electrode would be more strongly attracted outward from the electrode for smaller d , and d_{es}^+ would be a decreasing function of d . However, the calculated results show that d_{es}^+ is surely an increasing function of d .

The d dependence also provides interesting information on the dielectric polarization effect. Since Q is proportional to E in classical electrostatics, the values of E must coincide with each other when the values of Q are the same for different μ and different d . From the above discussion, d_{es}^+ is governed by charge Q accumulated on the electrode and electric field E in the space between the electrodes. Therefore, the values of d_{es}^+ are expected to also be the same when the values of Q are the same for different μ and different d . According to Fig. 2(c), $Q = 3 \times 10^{-22}$ C/Å² for $\mu = 4.3$ eV at $d = 4.76$ Å and for $\mu = 5.4$ eV at $d = 7.94$ Å. If we check Fig. 4(a), $d_{\text{es}}^+ = 1.55$ Å when $\mu = 4.3$ eV at $d = 4.76$ Å, and $d_{\text{es}}^+ = 1.59$ Å when $\mu = 5.4$ eV at $d = 7.94$ Å. Therefore, the two values of d_{es}^+ do not coincide and the classical picture breaks down. This paradox can be explained by the fact that smaller d has larger E . This clearly means that the relation between Q and E is different if d is different, namely, that the proportionality coefficient, the effective dielectric constant of the space between the electrodes, ϵ , is a function of d . This seems to be related with the slightly decreasing ϵ_{eff} when μ increases as discussed in the previous section [Fig. 3(c)]. Thus, simple geometrical theory based on classical electrostatics is not useful for nanocapacitance.

If we further analyze the calculated results for d_{es}^\pm more carefully, we find that the degrees of the μ dependence of d_{es}^+ and of d_{es}^- are different. Since the directions of the μ dependence of d_{es}^\pm are opposite, such a difference can be more clearly found in the dependence of d_{es} , which is calculated as $d_{\text{es}} = 2b - (d_{\text{es}}^+ + d_{\text{es}}^-)$.

The d_{es} is shown in Fig. 4(c) as a function of μ , and in Fig. 4(d) as a function of d . The d_{es} decreases as μ increases. This means that d_{es}^- changes more rapidly than d_{es}^+ . Such a feature can be explained by the electronic states of the electrodes. Electrons are added to the conduction band in the negative electrode and removed from the valence band in the positive electrode. The wave functions of both the conduction and the valence bands are localized around the Si region; dielectric response should occur to reduce the Coulomb energy. Therefore, electrons move from Si to H in the negative electrode and from H to Si in the positive electrode. Since

Si-H antibonding states are not occupied, the electrons move into these states in the negative electrode. In addition, because the band energy of these states is close to the conduction band bottom, the electrons might move rather easily. On the other hand, the electrons move from the occupied Si-H bonding states in the positive electrode. Since the band energy of these states is far from the valence band top, the electrons might move with difficulty. Therefore, the μ dependence of d_{es}^- is more rapid than that of d_{es}^+ because of the dielectric polarization of the electrode materials. Here, we must also take into account the artifact of our EFED method. The suppression effect on d_{es}^- of the EFED well is thought to be large for small d .

In nanocapacitors, therefore, the classical picture is not true even for part of the electrostatic capacitance because of the dielectric polarization of the electrode materials. The electrode surface positions indicated by d_{es}^\pm cannot be fixed on a nanoscale, and it moves with electrode spacing d as well as with applied bias μ . Since d_{es}^\pm and d_{es} change with Q and μ , Eqs. (8) and (9) are not correct in nanocapacitors. The nonclassical effect of d_{es}^\pm and d_{es} is one order of the magnitude smaller than that of d_0 . These results are attributed to the moderate density of states and to the relatively low dielectric constant of the electrode material, planar polysilane, as well as to the narrow spacing between the electrodes. If electrodes are made of materials with larger density of states around the Fermi energy, or if electrode spacing is just wider, the quantum capacitance effect must be reduced. If electrodes are made of materials with a higher dielectric constant, the dielectric polarization effect must be enhanced. For a general nanocapacitor, the quantum capacitance effect and/or the dielectric polarization effect are thus thought to appear depending on the electronic feature of the electrode materials as well as the geometry of the nanocapacitor.

VI. CONCLUSION

We studied nonclassical features of a planar polysilane nanocapacitor by changing both electrode spacing d and applied bias μ simultaneously. We find that the effective electrode spacing d_0 decreases with μ even if d is fixed because of the effect of the quantum capacitance C^+ and C^- . In addition, when we analyze the electrostatic capacitance C_{es} in detail, we also find that the effective electrode surface positions indicated by d_{es}^\pm change complicatedly with d and μ because of the dielectric polarization effect of the electrode material. The dielectric polarization effect is one order of the magnitude smaller than the quantum capacitance effect, which is due to the nature of the electrode material, planar polysilane. We can conclude that a nanocapacitor is governed by the detailed properties of the electronic states of the electrode materials as well as the geometry.

ACKNOWLEDGMENTS

We thank Kazuyuki Uchida for his helpful comments. We also thank Hiroshi Inokawa and Hiroshi Yamaguchi for their helpful advice. A part of this study was supported by KAKENHI (22310062) from the Japan Society for the Promotion of Science.

*kageshima.hiroyuki@labs.ntt.co.jp

- ¹T. P. Smith, W. I. Wang, and P. J. Stiles, *Phys. Rev. B* **34**, 2995 (1986).
- ²V. Mosser, D. Weiss, K. von Klitzing, K. Ploog, and G. Weimann, *Solid State Commun.* **58**, 5 (1986).
- ³S. Luryi, *Appl. Phys. Lett.* **52**, 501 (1988).
- ⁴S. V. Kravchenko, D. A. Rinberg, S. G. Semenchinsky, and V. M. Pudalov, *Phys. Rev. B* **42**, 3741 (1990).
- ⁵J. P. Eisenstein, L. N. Pfeiffer, and K. W. West, *Phys. Rev. Lett.* **68**, 674 (1992).
- ⁶L. I. Glazman, I. M. Ruzin, and B. I. Shklovskii, *Phys. Rev. B* **45**, 8454 (1992).
- ⁷M. Büttiker, H. Thomas, and A. Prêtre, *Phys. Lett. A* **180**, 364 (1993).
- ⁸J. G. Hou, B. Wang, J. Yang, X. R. Wang, H. Q. Wang, Q. Zhu, and X. Xiao, *Phys. Rev. Lett.* **86**, 5321 (2001).
- ⁹M. M. Fogler, *Phys. Rev. Lett.* **94**, 056405 (2005).
- ¹⁰L. Latessa, A. Pecchia, A. DiCarlo, and P. Lugli, *Phys. Rev. B* **72**, 035455 (2005).
- ¹¹S. Ilani, L. A. K. Donev, M. Kindermann, and P. L. McEuen, *Nat. Phys.* **2**, 687 (2006).
- ¹²Z. Chen and J. Appenzeller, *Electron Devices Meeting 2008, IEDM '08*, Technical Digest (IEEE International, Piscataway, NJ, 2008), p. 509.
- ¹³H. Xu, Z. Zhang, and L.-M. Peng, *Appl. Phys. Lett.* **98**, 133122 (2011).
- ¹⁴T. Christen and M. Büttiker, *Phys. Rev. Lett.* **77**, 143 (1996).
- ¹⁵J. Wang, H. Guo, J.-L. Mozos, C. C. Wan, G. Taraschi, and Q. Zheng, *Phys. Rev. Lett.* **80**, 4277 (1998).
- ¹⁶X. Zhao, J. Wang, and H. Guo, *Phys. Rev. B* **60**, 16730 (1999).
- ¹⁷M. Tanaka, Y. Gohda, S. Furuya, and S. Watanabe, *Jpn. J. Appl. Phys.* **42**, L766 (2003).
- ¹⁸N. Nakaoka and K. Watanabe, *Eur. Phys. J. D* **24**, 397 (2003).
- ¹⁹K. Uchida, H. Kageshima, and H. Inokawa, *Phys. Rev. B* **74**, 035408 (2006).
- ²⁰K. Uchida, S. Okada, K. Shiraishi, and A. Oshiyama, *J. Phys.: Condens. Matter* **19**, 365218 (2007).
- ²¹K. Uchida, S. Okada, K. Shiraishi, and A. Oshiyama, *Phys. Rev. B* **76**, 155436 (2007).
- ²²K. Uchida and S. Okada, *Phys. Rev. B* **79**, 085402 (2009).
- ²³K. Uchida and A. Oshiyama, *Phys. Rev. B* **79**, 235444 (2009).
- ²⁴K. Takeda and K. Shiraishi, *Phys. Rev. B* **39**, 11028 (1989).
- ²⁵C. G. Van de Walle and J. E. Northrup, *Phys. Rev. Lett.* **70**, 1116 (1993).
- ²⁶H. Kageshima and K. Shiraishi, *Phys. Rev. B* **56**, 14985 (1997).
- ²⁷J. Noborisaka, K. Nishiguchi, H. Kageshima, Y. Ono, and A. Fujiwara, *Appl. Phys. Lett.* **96**, 112102 (2010).
- ²⁸J. Noborisaka, K. Nishiguchi, Y. Ono, H. Kageshima, and A. Fujiwara, *Appl. Phys. Lett.* **98**, 033503 (2011).
- ²⁹H. Kageshima and A. Fujiwara, *Appl. Phys. Lett.* **96**, 193102 (2010).
- ³⁰H. Kageshima and A. Fujiwara, *Appl. Phys. Lett.* **93**, 043516 (2008).
- ³¹J. P. Perdew, K. Burke, and M. Ernzerhof, *Phys. Rev. Lett.* **77**, 3865 (1996).